International Journal Software Engineering and Computer Science (IJSECS)
6 (1), 2026, 257-267
Published Online April 2026 in IJSECS (http://www.journal.lembagakita.org/index.php/ijsecs)
P-ISSN: 2776-4869, E-ISSN: 2776-3242. DOI: https://doi.org/10.35870/ijsecs.v6i1.7143.

RESEARCH ARTICLE Open Access

Dual-Band Microstrip Antenna Design for 2.4 GHz and 5.3 GHz WiFi Networks

Muhammad Zainul Arifin [1*], **Syah Alam** [2]

[1*,2] Department of Electrical Engineering, Faculty of Industrial Technology, Universitas Trisakti, West Jakarta City, Special Capital Region of Jakarta, Indonesia.

**Corresponding author*: 162012310004@std.trisakti.ac.id.

Received: April 7, 2026; Accepted: April 15, 2026; Published: April 20, 2026.

Abstract: This study reports the design and simulation of a dual-band rectangular patch microstrip antenna intended for Wi-Fi applications at 2.4 GHz and 5.3 GHz. Initial patch dimensions were derived analytically at 2.4 GHz, then refined through an iterative optimization process involving the progressive insertion of vertical slots on the radiating patch. Three iterations were performed, each modifying slot length and width to shift the second resonant frequency toward the 5.3 GHz target while preserving the first resonance at 2.4 GHz. The finalized design resonated at approximately 2.49 GHz and 5.3 GHz, with return loss values of −16.11 dB and −15.5 dB, respectively — both satisfying the −10 dB threshold commonly adopted as the minimum criterion for acceptable antenna matching. VSWR values of 2.945 at 2.493 GHz and 2.613 at 5.3 GHz were recorded; these remain above the ideal upper bound of 2, indicating that impedance matching between the antenna and the feed line has not been fully resolved. Measured bandwidths were 143 MHz at 2.498 GHz and 2.8 MHz at 5.3 GHz, with the notably narrow bandwidth at the higher frequency representing a practical limitation that warrants further attention. Gain at 2.498 GHz reached 6.01 dBi, while the value at 5.2 GHz dropped to −4.369 dBi, suggesting that the slot geometry, though effective for frequency tuning, introduced radiation efficiency losses at the upper band. Taken together, the results confirm that vertical slot insertion is a viable technique for generating dual-band resonance in a rectangular patch microstrip antenna; the approach, however, requires additional refinement — particularly in impedance matching and upper-band gain recovery — before the design can be considered fully deployment-ready.

Keywords: Microstrip Antenna; Rectangular Patch; Return Loss; VSWR; Bandwidth; Gain.

1. Introduction

The antenna occupies a position in wireless communication systems that is difficult to overstate. As the physical interface between a guided transmission line and free space, it governs the conversion of electrical signals into propagating electromagnetic waves — and vice versa. Every measurable aspect of wireless link quality, from received signal strength to coverage radius to spectral efficiency, is conditioned in part by how well the antenna performs at its operating frequency. As microwave-frequency inter-device communication has grown from a niche application into the backbone of everyday connectivity, the antenna has moved from a peripheral hardware concern to a central design variable in modern telecommunication systems (Sabila *et al.*, 2018). The pressure on antenna designers has, accordingly, intensified — and the constraints they must satisfy have multiplied.

What makes antenna design genuinely difficult is that the requirements pulled from different directions rarely align neatly. A compact form factor tends to conflict with broad bandwidth. Low fabrication cost tends to conflict with tight impedance control. Ease of integration into a host device tends to conflict with radiation efficiency. The microstrip antenna has emerged as one of the more credible engineering responses to this set of tensions. Its planar geometry is compatible with standard printed circuit board manufacturing, its mass and volume are low, and its resonant frequency, polarization, and radiation pattern can each be adjusted by modifying patch geometry or substrate selection — without fundamentally altering the fabrication process (Akbar *et al.*, 2017). These properties have made microstrip antennas the subject of sustained research attention across the past three decades, and their deployment in commercial wireless devices is now routine. Among the available patch geometries — circular, triangular, annular ring, and rectangular — the rectangular patch has attracted the most consistent interest. The analytical framework relating patch width and length to resonant frequency through the substrate's effective permittivity is well-established, the fabrication process is among the simplest available, and the design equations are sufficiently transparent to support rapid iterative refinement (Susanto *et al.*, 2024). For a research context in which simulation-driven iteration is central to the design methodology, this tractability is not a minor convenience — it is a practical necessity.

The specific challenge addressed in this study is dual-band operation. Wi-Fi technology, as standardized under IEEE 802.11, operates across two primary frequency allocations: the 2.4 GHz band, spanning roughly 2.400–2.484 GHz, and the 5 GHz band, covering multiple sub-bands between approximately 5.150 and 5.850 GHz. A device operating across both bands either requires two separate antennas — adding mass, volume, and cost — or a single antenna capable of resonating at both frequencies simultaneously. The latter is clearly preferable in compact device design, but it is not straightforwardly achieved with a plain rectangular patch, which in its unmodified form supports only a single dominant resonance. Structural modification is required, and the choice of technique determines how much of the original patch's performance is preserved at the primary frequency while the second resonance is introduced. Slot insertion has been identified in the literature as one of the more controllable approaches for this purpose. By cutting a slot into the patch surface, the effective electrical length of the current path is altered, shifting the resonant frequency in a direction and by a magnitude that depends on slot geometry, orientation, and position relative to the feed point. With careful dimensioning, a second resonance can be placed at a target frequency without eliminating the first. Yosefariko (2015) demonstrated this principle using a U-shaped slot for dual-band Wi-Fi operation; the present study applies a vertical slot configuration to the 2.4 GHz and 5.3 GHz band pair — a combination that has received comparatively less attention than the 2.4 GHz and 3.6 GHz pairing addressed in earlier published work.

This study reports the design, iterative optimization, and simulation of a rectangular patch microstrip antenna for dual-band Wi-Fi operation at 2.4 GHz and 5.3 GHz. The design process began with analytical calculation of initial patch dimensions at 2.4 GHz, followed by three successive iterations in which vertical slot dimensions were progressively modified to shift the second resonance toward 5.3 GHz. Performance was evaluated at each stage through return loss, VSWR, bandwidth, and gain, with all simulation carried out in AWR Design Environment. The scope of the study is confined to simulation-based design and evaluation; physical fabrication and over-the-air measurement are not addressed here. The results are intended to contribute to the body of knowledge on slot-based dual-band microstrip antenna design for compact Wi-Fi applications, and to identify the specific performance gaps — particularly in VSWR and upper-band gain — that remain open for subsequent work (Yosefariko, 2015; Sabila *et al.*, 2018).

2. Literature Review

2.1 Antenna

An antenna is a transducer between a guided transmission structure and free space, designed to radiate or receive electromagnetic waves. In most practical configurations, the radiating element is fabricated from a conductive material — typically a metallic rod, wire, or printed trace — whose geometry determines how electromagnetic energy is distributed in space. Beyond simple radiation, an antenna also functions as a directive device: it concentrates radiated energy toward preferred directions while suppressing it in others, a property that directly affects link budget, interference management, and overall system efficiency (Kumar & Singh, 2023; World Bank, 2022).

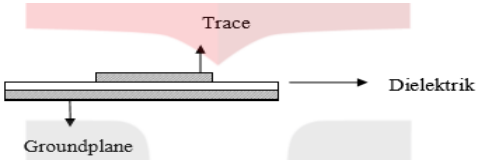

Figure 1. Antenna Structure

2.2 Microstrip Antenna

The microstrip antenna is a low-profile, planar radiating structure fabricated using printed circuit technology. It consists of a conductive patch printed on one face of a dielectric substrate, with a continuous ground plane on the opposite face. This configuration is mechanically simple, compatible with mass-production processes, and offers considerable flexibility in the adjustment of resonant frequency, polarization, radiation pattern, and input impedance — all through modification of patch geometry or substrate properties, without altering the fundamental fabrication approach (Balanis, 2016). Basic patch geometries include square, rectangular, circular, triangular, and circular ring forms, as illustrated in Figure 2. Among these, the rectangular patch is the most widely adopted, owing to the relative simplicity of its analytical design equations and the straightforwardness of its fabrication.

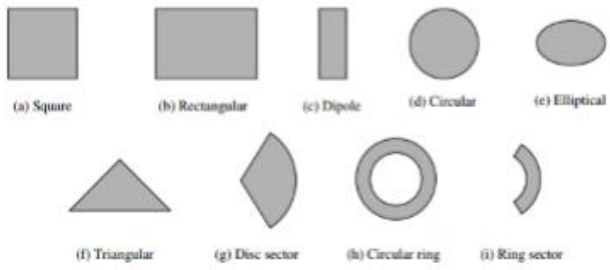

Figure 2. Antenna Patch Geometries

2.3 Input Impedance

Input impedance is the ratio of voltage to current at the antenna's feed terminal. Its value is not fixed; it varies with measurement position along the transmission line and with the structural characteristics of the antenna under consideration. In practice, input impedance determines the degree of matching between the antenna and its feed network — a mismatch at this interface results in reflected power, reduced radiation efficiency, and degraded system performance. Achieving a well-matched condition across the operating bandwidth is therefore a primary objective in antenna design (Abdullah *et al.*, 2024).

2.4 Voltage Standing Wave Ratio (VSWR)

VSWR is defined as the ratio of the maximum to minimum amplitude of the voltage standing wave pattern that forms along a transmission line when incident and reflected waves coexist. It is derived from the voltage reflection coefficient Γ, a complex quantity that encodes both the magnitude and phase of the reflected wave relative to the incident wave. A VSWR of 1 indicates perfect impedance matching with no reflected power; values above 2 are generally taken as indicative of significant mismatch and are considered unacceptable in most antenna applications.

2.5 Return Loss

Return loss is the ratio, expressed in decibels, of the amplitude of the reflected wave to that of the incident wave at a given port. It arises from impedance discontinuities between the transmission line and the antenna input terminal. A return loss more negative than −10 dB is the widely adopted threshold for acceptable antenna matching, corresponding to less than 10% of incident power being reflected. The frequency at which return loss reaches its minimum value identifies the antenna's resonant frequency and serves as the primary indicator of correct resonant behavior in simulation-based design.

2.6 Bandwidth

Bandwidth, in the context of antenna performance, refers to the range of frequencies over which the antenna meets a defined performance criterion — most commonly a return loss below −10 dB or a VSWR below a specified upper limit. It is not an intrinsic property of the antenna in isolation; it depends on which parameter is used to define it and at what threshold. For microstrip antennas, bandwidth is typically narrow relative to other antenna types, a consequence of the high Q-factor associated with the resonant patch structure. Bandwidth can be extended through substrate selection, patch geometry modification, or the introduction of additional resonant elements (Chen *et al.*, 2021; Rahman *et al.*, 2023).

2.7 Beamwidth

Beamwidth is measured from the antenna's far-field radiation pattern and describes the angular width of the main radiated lobe between the points at which power density falls to half its maximum value. For the Eθ component of a microstrip antenna, beamwidth narrows as the substrate relative permittivity ε_r increases beyond unity, while it broadens as the normalized substrate thickness h/a increases at $\varepsilon_r = 1$. This behavior

is a consequence of surface wave contributions, which become more pronounced at higher permittivity values and redistribute radiated energy away from the broadside direction.

2.8 Radiation Pattern

The radiation pattern of an antenna is a graphical representation of the spatial distribution of radiated power as a function of direction, typically evaluated in the far field. Microstrip antennas generally produce a broadside pattern, with maximum radiation directed normal to the patch surface. This characteristic is broadly consistent with that of many conventional antenna types, though the specific shape of the pattern — including sidelobe levels and cross-polarization — is sensitive to substrate thickness, permittivity, and patch geometry.

2.9 Polarization

Antenna polarization, in a specified direction, is defined as the polarization of the wave radiated in that direction when the antenna operates as a transmitter. Equivalently, when the antenna operates as a receiver, it refers to the polarization of an incident wave that produces maximum output power at the antenna terminals. For a standard rectangular microstrip patch fed along its length axis, the dominant polarization is linear, aligned with the direction of the feed.

2.10 Rectangular Microstrip Antenna Analysis

The rectangular microstrip antenna consists of three principal components: the radiating patch, the dielectric substrate, and the ground plane. Radiation occurs at the fringing fields that form at the open edges of the patch, where the confined electric field partially extends into the surrounding space and couples energy into free-space propagation. When the patch is excited through its feed, surface currents flow along the patch length and generate electromagnetic waves that propagate away from the structure. The dominant resonant mode is TM_{10}, in which the patch length is the primary determinant of resonant frequency, while the patch width influences radiation efficiency and input impedance. The principal dimensional parameters of a rectangular microstrip antenna are calculated as follows. Patch width W is a function of the operating frequency f_r, the speed of light c, and the substrate relative permittivity ε_r, and is given by:

$$W = \frac{c}{2f_r}\sqrt{\frac{2}{\varepsilon_r + 1}}$$

Patch length L is determined by the resonant frequency and must be corrected for the fringing field extension ΔL, which accounts for the fact that the effective electrical length of the patch exceeds its physical length. The correction depends on the effective permittivity $\varepsilon_e$ff, which reflects the partial confinement of the electromagnetic field within the dielectric substrate rather than entirely in free space:

$$L = \frac{c}{2f_r\sqrt{\varepsilon_{eff}}} - 2\Delta L$$

Where $\varepsilon_e$ff and ΔL are each functions of the substrate permittivity, thickness, and patch width. These equations provide the starting point for the design process; in practice, the initial dimensions derived from these expressions are subsequently refined through simulation to account for effects not captured by the analytical model, including feed reactance, substrate surface waves, and mutual coupling in slotted configurations.

3. Methodology

3.1 Design Workflow

The design and simulation process followed a structured sequential workflow, as illustrated in Figure 3. The procedure began with the selection of the patch geometry, followed by analytical calculation of initial dimensions at the target frequencies of 2.4 GHz and 5.3 GHz. The resulting design was then entered into simulation, where its performance was evaluated against the criteria of return loss < −10 dB and VSWR < 3. If the criteria were not met, the design was returned for dimensional revision and iterative slot modification. The process continued until both criteria were satisfied, at which point the design was considered finalized.

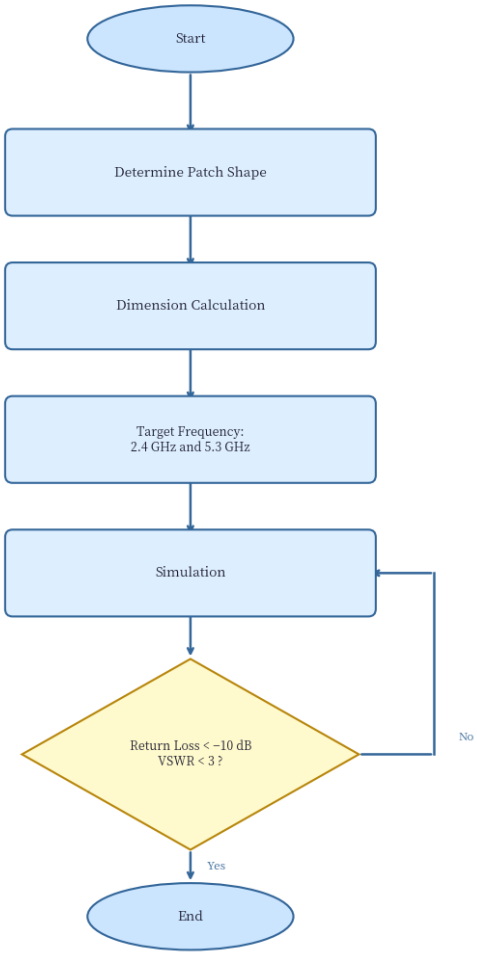

Figure 3. Design Workflow Flowchart

3.2 Determination of Patch Width and Length

Initial patch dimensions were derived analytically for a primary resonant frequency of 2.4 GHz, using a substrate with relative permittivity $\varepsilon_r = 4.3$ and thickness $h = 1.6$ mm. Patch width W was calculated using the standard transmission line model expression:

$$W = \frac{c}{2f_0}\sqrt{\frac{2}{\varepsilon_r + 1}} = \frac{3 \times 10^8}{2 \times 2.462 \times 10^9}\sqrt{\frac{2}{(4.3+1)}} = 0.037429 \text{ m} = 37.429 \text{ mm}$$

Where c is the speed of light in free space, f_0 is the operating frequency, and ε_r is the relative permittivity of the substrate. The result was rounded to W = 38 mm for implementation. The effective permittivity $\varepsilon_e$ff was then calculated to account for the partial confinement of the electromagnetic field within the dielectric substrate:

$$\varepsilon_{eff} = \frac{\varepsilon_r + 1}{2} + \frac{\varepsilon_r - 1}{2}\left(1 + \frac{12h}{W}\right)^{-1/2} = \frac{4.3 + 1}{2} + \frac{4.3 - 1}{2}\left(1 + \frac{12 \times 1.6}{37.429}\right)^{-1/2} = 3.495$$

The fringing field extension ΔL was subsequently computed as:

$$\Delta L = 0.412h\left(\frac{\varepsilon_{eff} + 0.3}{\varepsilon_{eff} - 0.258}\right)\left(\frac{\frac{W}{h} + 0.264}{\frac{W}{h} + 0.8}\right) = 0.412 \times 1.6\left(\frac{3.495 + 0.3}{3.495 - 0.258}\right)\left(\frac{\frac{37.429}{1.6} + 0.264}{\frac{37.429}{1.6} + 0.8}\right) = 0.754 \text{ mm}$$

Patch length L was then determined by:

$$L = \frac{c}{2f_0\sqrt{\varepsilon_{eff}}} - 2\Delta L = \frac{3 \times 10^8}{2 \times 2.462 \times 10^9 \times \sqrt{3.495}} - 2 \times 0.754 = 32.59 \text{ mm} - 1.508 \text{ mm} = 31.082 \text{ mm}$$

The analytical calculation yielded W = 37.429 mm (rounded to 38 mm) and L = 31.082 mm. In the actual simulation, the patch length was adjusted to 29 mm following preliminary simulation results, which indicated that a slight dimensional reduction was necessary to bring the resonant frequency into closer alignment with the 2.4 GHz target — a common outcome when fringing field corrections alone do not fully account for feed reactance and substrate edge effects.

3.3 Antenna Design

Following the analytical calculation and preliminary simulation, the patch dimensions were finalized at W = 38 mm and L = 29 mm, with a feed line width of 3 mm. The resulting patch geometry is shown in Figure 4. The substrate material was specified with ε_r = 4.3 and h = 1.6 mm, consistent with the parameters used in the dimensional calculation. These dimensions served as the baseline configuration from which iterative slot modifications were subsequently applied to achieve dual-band operation.

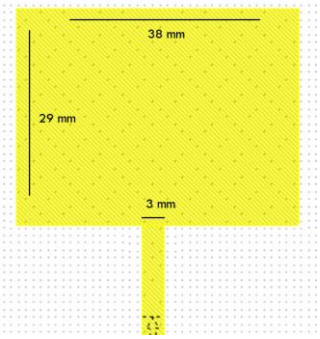

Figure 4. Antenna Design Configuration

3.4 Simulation Process in AWR Design Environment

All simulation work was carried out in AWR Design Environment, following a three-stage procedure. In the first stage, the substrate layer thickness and dielectric constant were specified to define the material properties of the simulation environment. In the second stage, the patch geometry and dimensions were entered, establishing the baseline single-band antenna model. In the third stage, vertical slot structures were introduced at designated positions on the patch surface, and their effect on the resonant frequency response was evaluated through successive iterations. At each iteration, return loss and VSWR were extracted from the simulation and compared against the design criteria, with slot dimensions adjusted incrementally until the dual-band target at 2.4 GHz and 5.3 GHz was approached.

4. Result and Discussion

4.1 Results

4.1.1 Optimization and Iteration Results

The operating frequency of the antenna was identified from the simulated return loss response, with the resonant frequency corresponding to the minimum return loss value at each iteration stage. Table 1 presents the simulation results for the baseline design and the first iteration, capturing the initial state of the antenna before any slot modification was applied.

Table 1. Simulation Results: Baseline and First Iteration

Data	Frequency (GHz)	Return Loss (dB)	VSWR
Baseline	2.402	−17.56	2.88
Baseline	4.996	−22.32	1.962
Iteration 1	2.443	−11.93	4.458
Iteration 1	5.008	−14.99	2.94

In the baseline configuration — corresponding to the plain rectangular patch described in Section 3 — the antenna resonated at 2.402 GHz and 4.996 GHz. While the return loss values at both frequencies satisfied the −10 dB threshold, the second resonance fell approximately 300 MHz below the 5.3 GHz target, and the overall frequency pair did not align with the intended Wi-Fi band combination. Structural modification was therefore necessary. The proposed iterative design sequence is shown in Figure 5, which illustrates the progressive slot modifications applied across all three iterations.

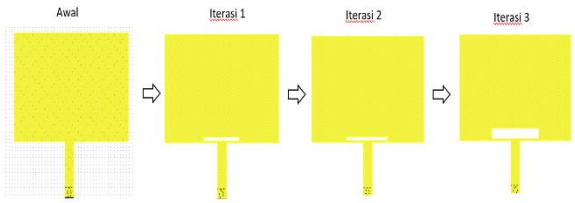

Figure 5. Proposed Antenna Design Iterations (Baseline → Iteration 1 → Iteration 2 → Iteration 3)

A horizontal slot was introduced on the lower portion of the patch, positioned 0.5 mm from the feed edge, with slot dimensions L = 1 mm and P = 12 mm, as shown in Figure 6. This modification shifted the second resonant frequency upward from 4.996 GHz to 5.008 GHz — a modest but directionally consistent response. The slot altered the effective current path length on the patch surface, which is the expected mechanism for slot-induced frequency tuning (Akbar *et al.*, 2017). The first resonance shifted slightly to 2.443 GHz, remaining within the 2.4 GHz Wi-Fi band. VSWR at the first resonance, however, rose to 4.458 — a notable deterioration relative to the baseline — indicating that the slot introduction disrupted the impedance matching condition at the lower band.

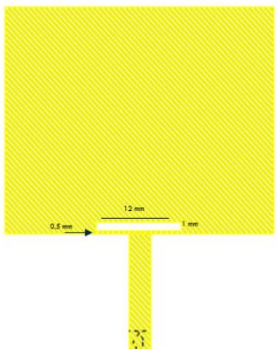

Figure 6. First Iteration — Slot Dimensions: L = 1 mm, P = 12 mm

The slot length was extended to P = 16 mm while the width was retained at L = 1 mm, as shown in Figure 7. This produced a more pronounced upward shift in the second resonance, reaching 5.1 GHz, and improved the VSWR at the upper band to 1.42. Return loss at 5.1 GHz reached −21.53 dB, well below the −10 dB threshold. At the lower band, the resonance settled at 2.5 GHz with a return loss of −11.93 dB, though VSWR remained at 3.92. The second iteration confirmed that slot length is the more sensitive parameter for controlling the upper resonant frequency, while its effect on lower-band impedance matching is less straightforward.

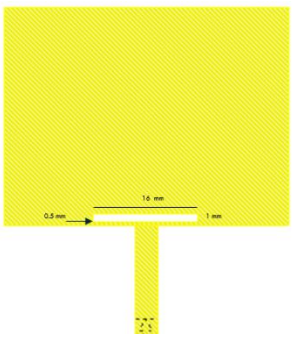

Figure 7. Second Iteration — Slot Dimensions: L = 1 mm, P = 16 mm

The slot width was increased to L = 2 mm with P = 16 mm retained, as shown in Figure 8. This final adjustment shifted the second resonance to 5.3 GHz — the intended target — while the first resonance remained at 2.498 GHz. Return loss values of −15.9 dB at 2.498 GHz and −16.6 dB at 5.3 GHz both satisfied the −10 dB criterion. VSWR values of 2.945 and 2.613 at the respective bands remained above the ideal threshold of 2, but the dual-band objective was met in terms of resonant frequency alignment.

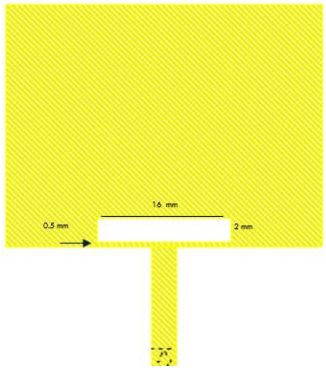

Figure 8. Third Iteration — Slot Dimensions: L = 2 mm, P = 16 mm

4.1.2 Gain and Bandwidth

Gain was extracted from simulation across the frequency range of 2–6 GHz, as shown in Figure 9. At 2.499 GHz, the antenna produced a gain of 6.011 dBi — a value consistent with expectations for a single rectangular patch operating in its dominant TM_{10} mode. At 5.308 GHz, the gain dropped sharply to −4.389 dBi. Negative gain at the upper band indicates that the slot geometry, while effective for frequency shifting, introduced current discontinuities on the patch surface that reduced radiation efficiency at 5.3 GHz. Some portion of the input power at this frequency is likely being dissipated or reflected rather than radiated — a known risk in slot-based dual-band designs where the same structural feature responsible for creating the second resonance can simultaneously degrade the patch's radiation behavior.

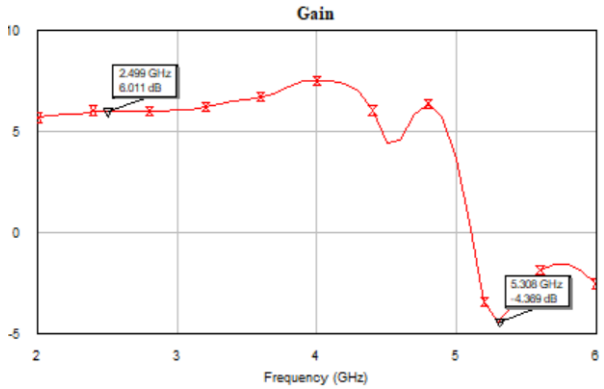

Figure 9. Simulated Gain vs. Frequency

Bandwidth was determined from the return loss response shown in Figure 10, using the −10 dB criterion. At 2.498 GHz, the antenna exhibited a bandwidth of 143 MHz, spanning from approximately 2.431 GHz to 2.574 GHz — a range that comfortably covers the 2.4 GHz Wi-Fi channel allocation. At 5.3 GHz, the bandwidth was only 2.8 MHz, spanning from approximately 5.282 GHz to 5.391 GHz. Standard Wi-Fi channel bandwidths at 5 GHz are 20 MHz or wider under IEEE 802.11a/n/ac; a 2.8 MHz bandwidth is insufficient for practical deployment and reflects the high Q-factor of the slot-induced upper-band resonance.

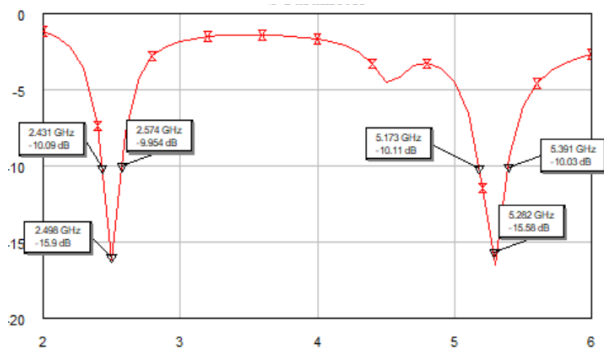

Figure 10. Simulated Return Loss — Final Design (Iteration 3)

4.1.3 Comparative Analysis Across Iterations

The full simulation results across all design stages are compiled in Table 2, and the return loss and VSWR progression across iterations are shown in Figures 11 and 12, respectively.

Table 2. Comparative Simulation Results Across All Iterations

Data	Frequency (GHz)	Return Loss (dB)	VSWR
Baseline	2.402	−17.56	2.88
Baseline	4.996	−22.32	1.962
Iteration 1	2.443	−11.93	4.458
Iteration 1	5.008	−14.99	2.94
Iteration 2	2.500	−11.93	3.92
Iteration 2	5.100	−21.53	1.42
Iteration 3	2.498	−15.90	2.945
Iteration 3	5.300	−16.60	2.613

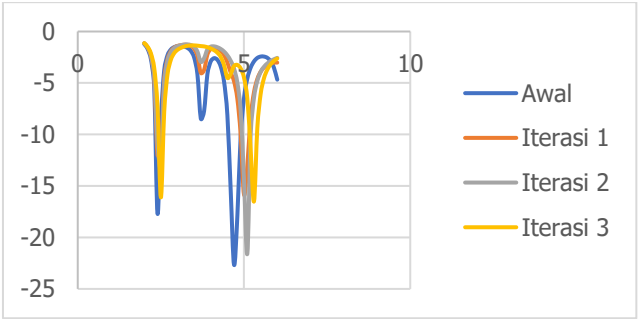

Figure 11. Return Loss Optimization Across Iterations

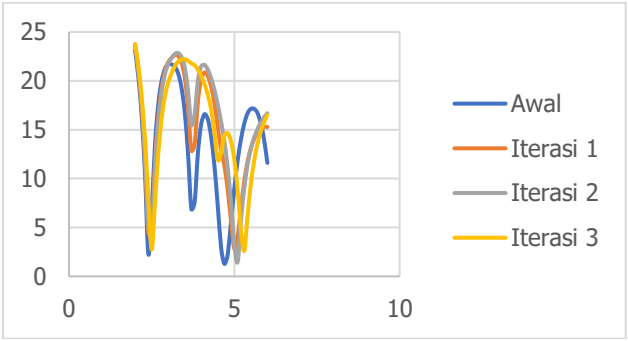

Figure 12. VSWR Optimization Across Iterations

The return loss curves in Figure 11 show a consistent rightward shift of the second resonance dip across iterations, from 4.996 GHz in the baseline to 5.3 GHz in the third iteration — a total shift of approximately 304 MHz achieved through slot dimension adjustments alone. The first resonance remained relatively stable across all iterations, drifting by no more than 100 MHz from the baseline value, confirming that the slot modifications were more influential on the upper-band resonance than on the lower. The VSWR curves in Figure 12 reveal a more mixed trajectory: while the upper-band VSWR improved substantially between iterations one and two (from 2.94 to 1.42), the third iteration saw it rise again to 2.613 as the slot width was increased. This trade-off between frequency alignment and impedance matching is a recurring challenge in slot-based dual-band design and points to the need for a more systematic co-optimization of slot geometry and feed network parameters in future work.

4.2 Discussion

The simulation results confirm that geometric optimization through iterative slot insertion plays a decisive role in shaping the dual-band resonant behavior of the rectangular patch antenna. Return loss served as the primary resonance indicator throughout — a standard and appropriate choice for this class of design (Balanis, 2016; Sabila *et al.*, 2018). What the results also reveal, however, is that slot-based tuning involves real trade-offs that are not always visible from the return loss curve alone. Before any modification, the plain rectangular patch produced two resonances, but neither aligned precisely with the target frequencies. The surface current distribution of an unmodified patch does not naturally support two well-separated, independently controllable resonances at 2.4 GHz and 5.3 GHz simultaneously. The introduction of a vertical slot in the first iteration changed the current path geometry and produced a measurable upward shift in the second resonance — consistent with the slotting mechanism documented by Akbar *et al.* (2017). The sensitivity of the resonant frequency to slot length, observed between iterations one and two, suggests that P is the more effective tuning parameter for the upper band, while slot width L has a secondary but non-negligible effect on both frequency alignment and impedance matching.

The VSWR results across iterations reveal a persistent matching problem. Even in the final iteration, VSWR values of 2.945 and 2.613 at the two bands indicate that reflected power remains non-trivial. A VSWR of 2.945 corresponds to a reflection coefficient magnitude of approximately 0.49, meaning that roughly 24% of incident power at 2.498 GHz is reflected rather than radiated. For a Wi-Fi application, this level of mismatch would reduce link efficiency and could require compensation at the transceiver level. The root cause is likely the absence of a dedicated impedance matching network; the feed line alone, at 3 mm width, may not provide sufficient matching across both bands simultaneously. Inset feed techniques, L-shaped matching stubs, or quarter-wave transformers could each address this in subsequent design iterations. The gain disparity between the two bands — 6.011 dBi at 2.499 GHz versus −4.389 dBi at 5.308 GHz — is the most practically significant result in this study. A gain of 6.011 dBi at the lower band is reasonable and consistent with published values for single rectangular patches of similar dimensions (Balanis, 2016). The negative gain at 5.3 GHz, by contrast, indicates that the antenna is not functioning as an efficient radiator at the upper band. The slot geometry that enables the second resonance appears to be disrupting the surface current distribution in a way that reduces radiation efficiency at that frequency. This is not an uncommon outcome in slot-based dual-band designs, and it points to a fundamental limitation of the approach when applied without simultaneous optimization of the radiation mechanism. The bandwidth result at 5.3 GHz — 2.8 MHz — compounds this concern further. A 2.8 MHz operational bandwidth is inadequate for any practical Wi-Fi channel, and it suggests that the upper-band resonance is highly resonant but poorly coupled to free space. Addressing this would likely require a more complex slot geometry, a thicker or lower-permittivity substrate, or the addition of a parasitic element to broaden the upper-band response (Yosefariko, 2015; Sabila *et al.*, 2018).

5. Conclusion

Based on the simulation results and optimization process carried out in this study, a single rectangular patch microstrip antenna with vertical slot insertion was demonstrated to operate at two distinct frequencies consistent with the target Wi-Fi application bands. The finalized design produced return loss values of −16.11 dB at 2.49 GHz and −15.5 dB at 5.3 GHz, both satisfying the −10 dB threshold that defines acceptable antenna matching in standard design practice. These results confirm that slot insertion on a single rectangular patch constitutes an effective structural approach for generating dual-band resonant behavior without requiring multiple radiating elements or a complex feed network. Although the dual-band frequency targets were achieved, the VSWR values obtained — 2.945 at 2.493 GHz and 2.613 at 5.3 GHz — remained above the ideal upper bound of 2. This indicates that impedance matching between the antenna and the 50 Ω transmission line has not been fully resolved, and that a non-negligible portion of incident power continues to be reflected rather than radiated at both operating frequencies. In comparison with prior studies that have predominantly addressed dual-band Wi-Fi antenna designs covering the 2.4 GHz and 3.6 GHz band combination, the present work extends the scope to the 2.4 GHz and 5.3 GHz pairing, which is more directly applicable to contemporary IEEE 802.11a/n/ac network deployments. The iterative slot-based optimization approach employed in this study successfully achieved the target frequency alignment through three successive and electromagnetically interpretable dimensional refinements. It is acknowledged that the design has not reached its full performance potential. The VSWR values above 2 at both bands, the negative gain of −4.389 dBi at 5.3 GHz, and the upper-band bandwidth of only 2.8 MHz collectively indicate that considerable room for improvement remains. Further performance gains may be pursued through the introduction of more complex slot configurations such as U-shaped or L-shaped slots, adjustment of substrate permittivity and thickness, or the incorporation of a dedicated impedance matching network, all of which represent viable directions for subsequent research.

References

Abdullah, A., Rahmani, K. R., Wadeed, W. M., & Hakimi, M. (2024). Data transfer security in IoT communication based on attribute-based cryptography. *International Journal of Software Engineering and Computer Science*, *4*(2), 553–565. https://doi.org/10.35870/ijsecs.v4i2.2887

Akbar, A., Alam, S., & Surjati, I. (2017). Perancangan antena mikrostrip patch circular (2,45 GHz) array dengan teknik pencatu proximity sebagai penguat sinyal Wi-Fi. *Setrum: Sistem Kendali-Tenaga-Elektronika-Telekomunikasi-Komputer*, *6*(2), 215–223. https://doi.org/10.36055/setrum.v6i2.2599

Balanis, C. A. (2016). *Antenna theory: Analysis and design* (4th ed.). Wiley.

Chen, W., Zhang, Y., & Liu, H. (2021). Dynamic waste collection optimization using real-time data analytics. In *Proceedings of the 2021 IEEE International Conference on Smart Cities* (pp. 234–241). IEEE Press.

Kumar, S., & Singh, R. (2023). Health impacts of inadequate waste management in developing countries: A meta-analysis. *Environmental Health Perspectives*, *131*(4), 047001. https://doi.org/10.1289/EHP11234

Rahman, M. A., Hossain, S., & Ahmed, T. (2023). Optimizing waste bin placement using K-means clustering: A case study of Dhaka city. *Waste Management & Research*, *41*(2), 456–468. https://doi.org/10.1177/0734242X221145678

Sabila, L. Y., Prakoso, T., & Sofwan, A. (2018). Perancangan antena mikrostrip circular patch untuk WiFi menggunakan characteristic mode analysis (CMA). *Transient*, *7*(1), 13–19. https://doi.org/10.14710/transient.7.1.13-19

Susanto, R. B., Rahayu, I., Permana, D., & Wibowo, A. (2024). Perancangan dan realisasi wearable antenna microstrip 2.4 GHz untuk memonitor pernapasan. *e-Proceeding of Engineering*, *11*(2), 1374–1377.

World Bank. (2022). *What a waste 2.0: A global snapshot of solid waste management to 2050*. World Bank Publications. https://openknowledge.worldbank.org/handle/10986/30317

hYosefariko. (2015). Design and realization dual-band microstrip antenna using U-shaped slot for WiFi application. *Perancangan dan Realisasi Antena Mikrostrip Dual-Band Menggunakan Slot Berbentuk U untuk Aplikasi WiFi*, *2*(2), 1–8.